agronomy

MDPI

*Article*

# Optimization of Litchi Fruit Detection Based on Defoliation and UAV

**Jing Wang [1], Mingyue Zhang [2], Zhenhui Zheng [3], Zhaoshen Yao [2], Boxuan Nie [4], Dongliang Guo [1], Ling Chen [2], Jianguang Li [1,*] and Juntao Xiong [2,*]**

[1] Key Laboratory of South Subtropical Fruit Biology and Genetic Resource Utilization, Guangdong Provincial Key Laboratory of Science and Technology Research on Fruit Trees, Institute of Fruit Tree Research, Guangdong Academy of Agricultural Sciences, Ministry of Agriculture and Rural Affairs, Guangzhou 510640, China; wangjing@gdaas.cn (J.W.); guodongliang@gdaas.cn (D.G.)
[2] College of Mathematics and Informatics, South China Agricultural University, Guangzhou 510642, China; zmyyyy@stu.scau.edu.cn (M.Z.); yzs790639993@gmail.com (Z.Y.); serenechen56@163.com (L.C.)
[3] Institute of Agricultural Machinery, Chinese Academy of Tropical Agricultural Sciences, Zhanjiang 524013, China; zhengzhenhui@catas.cn
[4] College of Horticulture, South China Agricultural University, Guangzhou 510642, China; nieboxuan@stu.scau.edu.cn
* Correspondence: lijianguang@gdaas.cn (J.L.); xiongjt@scau.edu.com (J.X.)

**Abstract**

The use of UAVs to detect litchi in natural environments is imperative for rapid litchi yield estimation and automated harvesting systems. However, UAV-based lychee fruit detection bottlenecks arise from complex canopy architecture and leaf occlusion. This study proposed a collaborative optimization strategy integrating agronomic technique with deep learning. Three leaf thinning intensities (0, 6, and 12 compound leaves) were applied at the early stage of fruit to systematically evaluate their effects on fruit growth, canopy structure, and detection performance. Results indicated that moderate defoliation (six leaves) significantly enhanced canopy openness and light penetration without adversely impacting on yield and fruit quality. Subsequent UAV-based detection under moderate versus no defoliation treatment revealed that the YOLOv8-based model achieved significant performance gains: mean average precision (mAP) increased from 0.818 to 0.884, and the F1-score improved from 0.796 to 0.842. The study contributes a novel collaborative optimization strategy that effectively mitigates occlusion issues in fruit detection. This approach demonstrates that agronomic techniques can be strategically used to enhance AI perception, offering a significant step forward in the integration of agricultural machinery and agronomy for intelligent orchard systems.

**Keywords:** Litchi; fruit detection; defoliation; UAV; YOLOv8

Academic Editor: Marco Fontanelli

Received: 14 August 2025
Revised: 22 September 2025
Accepted: 1 October 2025
Published: 19 October 2025

**Citation:** Wang, J.; Zhang, M.; Zheng, Z.; Yao, Z.; Nie, B.; Guo, D.; Chen, L.; Li, J.; Xiong, J. Optimization of Litchi Fruit Detection Based on Defoliation and UAV. *Agronomy* **2025**, *15*, 2421. https://doi.org/10.3390/agronomy15102421

**Copyright:** © 2025 by the authors. Licensee MDPI, Basel, Switzerland. This article is an open access article distributed under the terms and conditions of the Creative Commons Attribution (CC BY) license (https://creativecommons.org/licenses/by/4.0/).

## 1. Introduction

Lychee (*Litchi chinensis* Sonn.) represents an economically important fruit crop in southern China, and the fruit is attractive in the international market [1]. Its production is characterized by pronounced seasonality, concentrated yield pattern, and narrow harvesting window. Historically dependent on manual harvesting, conventional approaches have become increasingly unsustainable amidst persistently rising labor costs and work-

force shortages [2]. Consequently, developing efficient and robust fruit detection and harvesting assistance technologies has emerged as a critical imperative for industry modernization. Particularly during mid-to-late fruit development stages, the rapid and accurate acquisition of spatial distribution data constitutes an essential foundation for yield estimation and harvest strategy optimization, while serving as a fundamental prerequisite for advancing automated harvesting systems.

Recent advances in computer vision have led to the extensive application of convolutional neural network (CNN)-based object detection algorithms in fruit recognition tasks [3,4]. Sa et al. (2016) merged multi-modal color (RGB) and near-infrared (NIR) information based on a Faster R-CNN detector for fruit detection [5]. A YOLOv5 model combined with ShuffleNet v2 network can segment litchi fruit and stem pixels, and the average accuracy of litchi fruit detection by this method was 98.79% [6]. Zhou et al. (2023) used YOLOv7 to locate and classify dragon fruit, and proposed a PSP-elliptic method to further detect the endpoints of dragon fruit [7]. The accuracy, recall rate, and average accuracy were 0.844, 0.924, and 0.932, respectively. Tang et al. (2023) proposed YOLO-Oleifera based on improved YOLOv4-tiny model and binocular stereo vision, and it achieved an AP of 92.07% with an average of 31 ms to detect each fruit image [8].

However, most existing studies rely predominantly on close-range imagery or stationary ground-based platforms, with models typically deployed through manual data collection or vehicle-mounted systems. These approaches exhibit inherent limitations including suboptimal operational efficiency, restricted mobility, and strong dependence on orchard terrain conditions [9]. In contrast, low-altitude UAV aerial photography has gradually been favored due to its advantages such as flexible and convenient operation, low cost, high imaging resolution, and wide application range [10]. Zhao et al. (2021) used unmanned aerial vehicles to conduct multispectral detection of plant and head features for sorghum [11]. Li et al. (2022) detected and counted maize seedlings under complex background by UAV [12]. Xiong et al. (2022) proposed a method that combines drones with deep learning to detect individual fruit trees and map their spatial distribution [13]. Liu et al. (2025) used drone hyperspectral image data to monitor potato growth and estimate yield, verifying the effectiveness of CGMI and its close relationship with yield [14]. Cruz-Grimaldo et al. (2025) used UAV and multispectral sensor to conduct high-throughput phenotypic analysis on the plant height, yield, spectral characteristics, and other agricultural morphological characteristics of Peruvian cotton varieties, and established the yield prediction equation, which provided a powerful tool for germplasm evaluation and decision-making [15]. Orlandi et al. (2025) developed a rapid automated method based on UAV digital image analysis, and used a linear regression model to convert image data into yield for vineyard yield estimation [16]. Liang et al. (2025) made contributions through their YOLOv7-MSRSF framework, achieving 89.16–97.79% precision across three challenging scenarios (occlusion, overlap, illumination variation) and 96.1% mAP@0.5 using a novel UAV dataset [17]. Although related research has made progress in target detection, there are still fundamental limitations in practical application. Most of the work focuses on algorithm optimization (such as super-resolution, multi-scale feature fusion, model compression), but the impact of sensing conditions on detection performance is not enough. In complex scenes such as occlusion and small targets, the existing methods still perform poorly. Lin et al. (2025) proposed an improved yolov8 target detection algorithm dpd-yolo, which effectively improved the performance of pineapple detection under occlusion in complex background mAP@0.5. The accuracy, recall rate, and F1-score were improved by 2.7%, 13%, and 10.3%, respectively [18]. Teng et al. (2025) proposed an end-to-end micro target multi-scale feature extraction and fusion detection network, stff-rtdetr, to improve the performance of micro target detection in UAV images [19]. However, these studies are mostly limited to the improvement of model structure, and have

not yet taken "defoliation intervention" as an experimental variable to systematically explore its effect on image visibility and detection performance. This paper is to make up for this deficiency, and provides a new perspective and data support for agricultural detection practice by comparing the performance of UAV detection under the condition of defoliation and non-defoliation.

The complex canopy architecture and dense foliage of lychee trees frequently result in fruit occlusion by branches and leaves. This persistent challenge severely limits detection efficacy, as even advanced models with strong representational capacity cannot consistently detect fruits with insufficient exposure. Existing studies confirm that occlusion constitutes a primary contributor to reduced detection accuracy and elevated miss rates in orchard environments [20]. Nevertheless, this issue was predominantly framed as a 'computer vision challenge,' overlooking the inherent modifiability of tree architecture itself. Consequently, developing agronomic interventions to proactively optimize visual conditions and mitigate perceptual barriers at their source represents a critical pathway for addressing occlusion-related limitations.

Within fruit tree management, moderate defoliation serves as a well-established agronomic practice for regulating canopy ventilation, light penetration, and fruit quality parameters, extensively employed in crops including grapevines and apple trees. Research demonstrates that strategic thinning of basal foliage effectively reduces canopy leaf area index (LAI) while maintaining yield, enhances photosynthetically active radiation (PAR) within the canopy interior, and consequently improves sugar accumulation, coloration, and developmental quality of fruits [21,22]. Although these have primarily investigated defoliation's effects on physiological fruit traits, its potential impact on enhancing image-based fruit visibility and perception accuracy remains systematically unvalidated and quantitatively unassessed.

This study therefore proposed an integrated methodology synergizing agronomic structural intervention with computer vision optimization. By implementing moderate defoliation treatments during early lychee fruit stage, we aim to enhance image acquisition conditions for target fruits, and ultimately elevate UAV-based fruit detection performance. The specific research objectives are as follows:

(1) Implement three defoliation intensities during early fruit development (control: no leaf thinning; moderate: thinning of 6 compound leaves; intensive: thinning of 12 compound leaves), systematically evaluating their comprehensive effects on fruit growth dynamics, yield parameters, quality attributes, and canopy structural reorganization.
(2) Following identification of the optimal intervention level (moderate defoliation), acquire UAV-based imagery of control and moderate defoliation groups to construct a dedicated fruit detection dataset.
(3) Employ a YOLOv8 object detection framework to quantify recognition capability differences across canopy openness treatments.
(4) Investigate synergistic mechanisms between agronomic structural regulation and computer vision perception systems, establishing theoretical foundations and technical pathways for intelligent orchard monitoring frameworks.

## 2. Materials and Methods

### *2.1. Field Experimental Design and Agronomic Trait Quantification*

#### 2.1.1. Plant Material Specifications and Experimental Defoliation Design

Experiments were conducted during 2022–2024 in the lychee demonstration orchard of Fruit Tree Research Institute—Guangdong Academy of Agricultural Science, China

(23°14′ N, 113°36′ E). Fifteen-year-old 'Guiwei' lychee (*Litchi chinensis* Sonn. cv. Guiwei) trees with uniform vigor were selected.

Trees were planted in north–south orientation with 4.5 × 4.5 m spacing, averaging 3.5 m in height. Eight trees per treatment (24 total) were randomly assigned to three defoliation regimens applied at fruit set initiation (early April): (1) control (CK): no leaf defoliation; (2) moderate defoliation (T1): thinning of 6 compound leaves from the basal position of fruit-bearing shoots; (3) intensive defoliation (T2): thinning of 12 compound leaves from the basal position of fruit-bearing shoots. Defoliation targeted proximal subtending leaves immediately below fruit clusters without damaging apical meristems. Representative fruit-bearing shoots per tree were tagged for all subsequent measurements (Figure 1a).

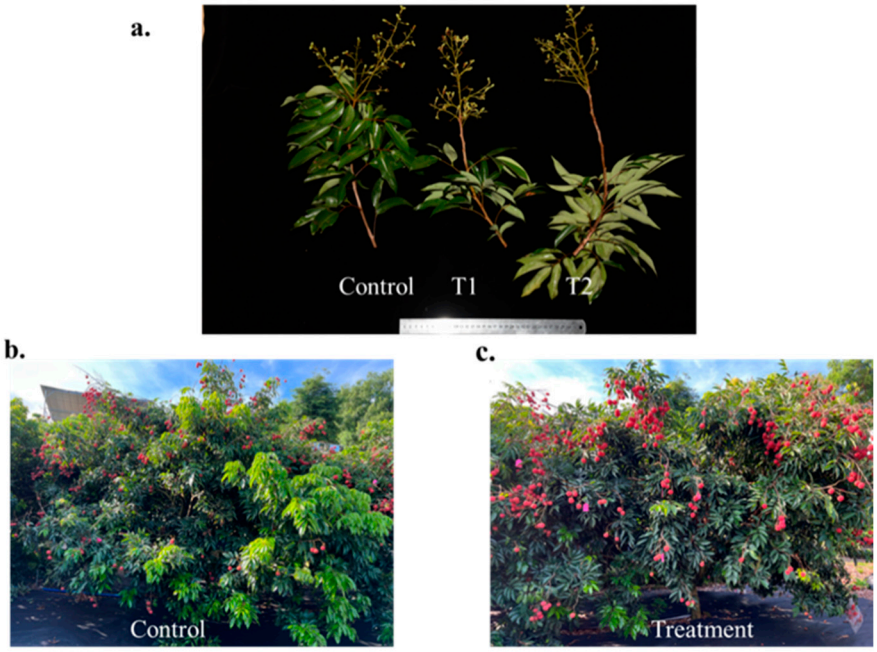



**Figure 1.** Example images of defoliation treatments. (**a**) Number of compound leaves thinning at young stage, with control as 0, T1 as 6, and T2 as 12; litchi without defoliation (**b**) and with defoliation (**c**) at maturity period.

#### 2.1.2. Determination of Fruit-Related Traits

To evaluate the effects of defoliation treatments on fruit settings, developmental dynamics, and final fruit quality, while determining whether perception optimization incurs yield or quality trade-offs. Systematic monitoring of lychee fruit development and maturation traits were implemented. During the fruit growth period (late April to mid-June), twenty fruiting branches were randomly selected from each tree to count the number of fruits per plantlet. The samples were collected every week per treatment. Randomly, one fruit per plantlet at each stage was selected. Eighty replicates were taken from fruits in four trees; the remaining four trees of each treatment were taken for the other evaluation. All samplings at each time point were performed in four biological repeats, and measured single fruit weight, fruit longitudinal and transverse meridians, seed weight, seed longitudinal and transverse diameters, pericarp thickness, and pulp thickness. The fruit setting rate from lychee plantlets was estimated by counting the number of fruits at seven-day intervals from the beginning of the fruit set until fruit maturing. The fruit soluble solids were measured by a portable brix meter PAL-1( ATAGO Co., Tokyo, Japan).

2.1.3. Measurement of Shoot Angle and Canopy Light Permeability

To assess whether defoliation treatment induced structural changes in shoots, potentially affecting fruit visibility and occlusion levels, four trees were randomly selected from each group (defoliated and control). From each tree, five fruit-bearing shoots were sampled from each of the four cardinal directions (east, south, west, north), resulting in a total of 80 shoots per group (4 trees × 4 directions × 5 shoots) subjected to curvature measurements. A self-made level used a transparent straw, closed both ends after being injected water, and the horizontal alignment of the plane was assessed by observing the position of the bubble within the straw. The level was the measuring tool, as shown in Figure 2; it was placed on the left and right sides of the fruiting mother litchi for pre-selection of photos. Then, the bending angle of the litchi shoot in the photo was accurately determined by using an angle ruler. The tortuosity of fruit stems was measured using a level as the horizontal plate line and litchi-bearing branches as the measurement datum. The specific measurement position was set 5–10 cm away from the top branch of the litchi. Samples were measured from 26 May to 21 June.




**Figure 2.** The illustrative image of angle ruler.

To further quantify the impact of defoliation treatment on canopy structural openness, the canopy characteristics of the lychee tree were measured using a CI-110 Plant Canopy Imager (CID Bio-Science, Inc., Camas, WA, USA). From 2022 to 2023, measurements were conducted at the beginning of April and May, with Sunday morning option. As shown in Figure 3, when operating, place the fisheye lens at three levels in the canopy and divide the zenith angle into three rings, with height above the ground as 1 m, 2 m, and 3 m, respectively. The azimuth angle was divided into six points, namely 0°, 45°, 135°, 180°, 225°, 315°; among them, each point was measured around a radius of 1 m with the trunk as the center, and then the average value was taken. The measured parameters include photosynthetically active radiation (PAR, μmol/m$^2$·s), leaf area index (LAI).

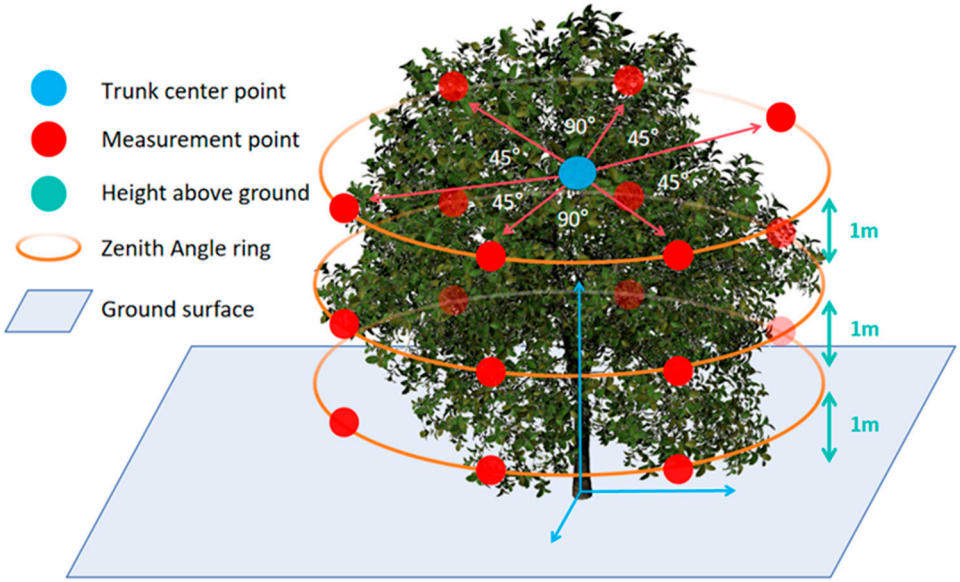



**Figure 3.** Diagram of the crown measurement point position as red dot.

#### 2.1.4. Statistical Analysis

All data were expressed as mean ± standard error. We used one-way analysis-of-variance (ANOVA) to examine differences. Calculate the value of the statistic F with the following formula:

$$\mathbf{F} = \frac{\mathbf{SSB/df(between)}}{\mathbf{SSW/df(within)}} \quad (1)$$

where SSB is the between-group fluctuation, SSW is the within-group fluctuation, specifically the number of groups minus one and the sum of the number of individuals in each group minus one. The least-significant-difference test (LSD) was performed when significant differences were detected by ANOVA for the west-facing slope. Significant differences were evaluated at a *p*-value of 0.01 level. All statistical analyses were performed using the software program SPSS, ver. 17.0 (SPSS Inc., Chicago, IL, USA).

### *2.2. UAV-Based Image Acquisition and Target Detection*

#### 2.2.1. Imaging Platform Deployment and Dataset Construction

To evaluate the impact of canopy defoliation on fruit visibility and UAV detection accuracy, a controlled field experiment and image acquisition campaign were conducted in a standardized litchi orchard at the Fruit Tree Research Institute in Guangzhou, China. Data collection was uniformly scheduled during the fruit ripening period in June. Four moderately defoliated trees (T1 treatment) and four control trees (CK) were selected. UAV imaging was performed using a DJI Phantom 4 Advanced drone (DJI, Shenzhen, China) equipped with a 1-inch CMOS sensor capable of capturing 4K video at 4096 × 2160 resolution. Individual trees were recorded separately, yielding eight aerial videos (four per treatment group).

Flights were conducted under clear weather conditions, with the UAV operating at approximately 2–3 m above the tree while slowly circumnavigating each tree to capture multi-angle views of the canopy. Each video lasted 1–2 min, with an average file size of ~2 GB. Videos from each group were randomly partitioned into training (50%), validation (25%), and test (25%) subsets, ensuring balanced representation across treatments. All quantitative metrics reported in the Results section were calculated on the independent test set, while the validation set was only used for hyperparameter tuning and overfitting monitoring. Keyframes were subsequently extracted from each video using uniform

frame sampling. The sampling frequency was optimized to maximize image diversity while minimizing redundancy, resulting in a total of 1000 high-resolution images. All images were resized to 2048 × 1080 pixels to maintain consistency and reduce computational overhead.

Fruit targets were annotated using LabelImg (available at https://github.com/tzutalin/labelImg), with bounding boxes delineating only the primary fruit body, irrespective of occlusion state.

#### 2.2.2. YOLO v8 Detection Model

The vision system is the core of agricultural UAV and crucial to ensure the accuracy and efficiency of litchi detection. Given the high complexity of litchi recognition, which included small target detection and issues with lighting conditions, this study proposed a litchi recognition model based on the YOLOv8 network. The YOLOv8 network structure is shown in Figure 4. The network mainly consisted of three parts: the backbone network (Backbone), the feature enhancement network (Neck), and the detection head (Head). Compared with other YOLO networks, YOLOv8 had the following improvements.

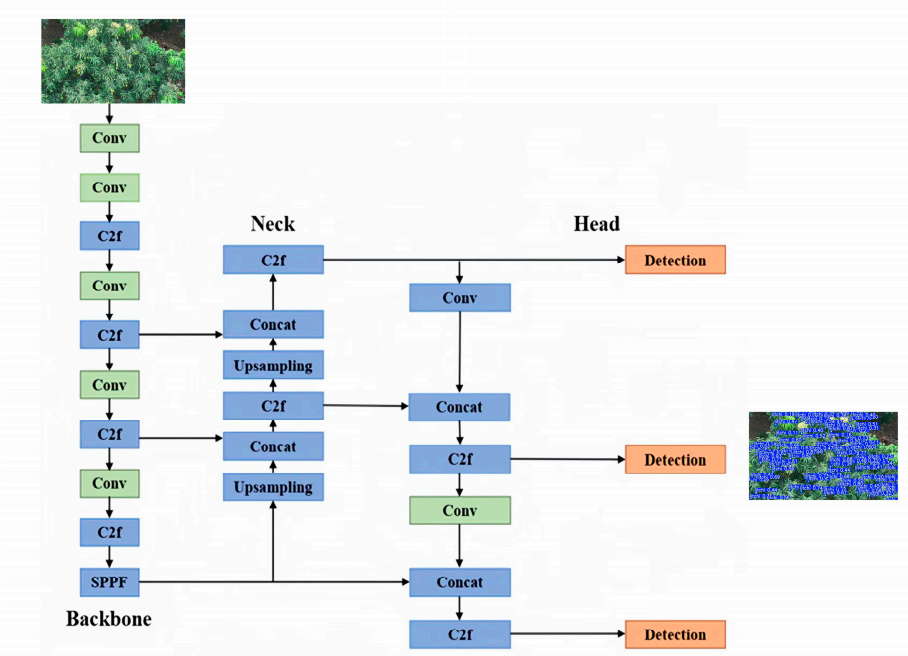



**Figure 4.** The overall structure of YOLOv8.

The backbone network of YOLOv8 was based on a faster CSP implementation. This module was inspired by the ELAN structure previously used in YOLOv7 [23]. The Cross Stage Partial (CSP) mainly featured traditional residual connections, whereas the C2f module, inspired by DenseNet [24], incorporated additional skip connections. It eliminated convolution operations within branches and introduced additional split operations. This not only enriched feature information but also reduced computational complexity. Additionally, YOLOv8 integrated the Spatial Pyramid Pooling Fast (SPPF) module, enhancing the model's ability to detect targets of various sizes. By lowering computational costs and merging outputs from each layer, SPPF maintained multi-scale feature integration and further expanded the model's receptive field. These improvements enhanced the model's ability to detect objects of different sizes while optimizing computational efficiency, meeting the performance requirements for litchi recognition in real-world environments.

2.2.3. Evaluation Metrics

The performance of the detection network largely determines the effectiveness of subsequent tasks such as fruit yield estimation. In this section, a comparative experiment was designed to verify the effectiveness of the proposed detection algorithm. Precision, recall, mAP, F1, and inference time are used as evaluation indicators, and the calculation formula was as follows:

$$\text{Precision} = \frac{\text{TP}}{\text{TP} + \text{FP}} \tag{2}$$

$$\text{Recall} = \frac{\text{TP}}{\text{TP} + \text{FN}} \tag{3}$$

$$\text{AP} = \sum_{k=1}^{N} P(k)\Delta\text{r(k)} \tag{4}$$

$$\text{F1} = \frac{2 * \text{Precision} * \text{Recall}}{\text{Precision} + \text{Recall}} \tag{5}$$

In the formula, TP represents the number of correctly detected fruits (true cases), FP represents the number of mistakenly detected fruits (false positive cases), and FN represents the number of missed fruits (false negative cases). P and R were precision and recall, respectively. AP represents the average precision at different recall rates, and mAP (mean average precision) is the mean value of AP across all categories. Inference time refers to the time required for a model to transition from input images to output predicted results. The shorter the inference time, the better the real-time performance of the model. F1 is the harmonic mean of precision and recall, which is an indicator reflecting the performance of the model. IoU (Intersection over Union) measures the overlap between the predicted bounding box and the ground truth bounding box, and is calculated as the area of their intersection divided by the area of their union. The higher the IoU value, the more accurate the predicted object location.

## 3. Results

### *3.1. Fruit Growth Monitoring*

Significant fruit abscission during early developmental stages, which severely compromises final yield, represents a major concern in orchard management [25]. To investigate the effects of defoliation treatments on fruit retention capacity and yield formation, fruit set dynamics and weight trajectories were systematically monitored from April to June.

As shown in Figure 5a, the most pronounced divergence in fruit set between treatment and control groups occurred during the early fruit development phase (circa 21 April). Notably, the T2 group exhibited accelerated fruit drop, characterized by rapid initial decline and prolonged duration, whereas T1 maintained relatively stable retention. By the conclusion of the abscission period (28 April), no significant differences in final fruit count persisted among treatments.

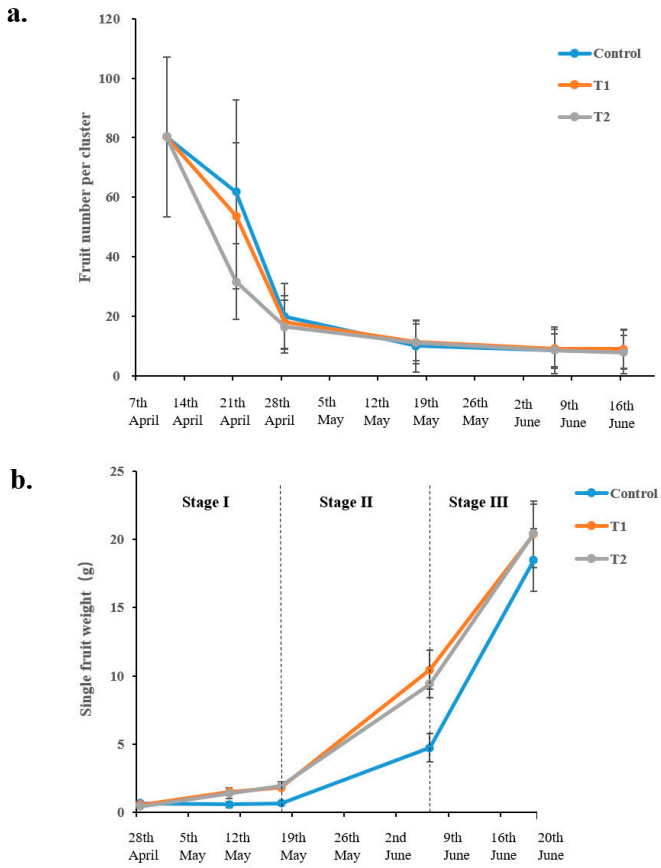



**Figure 5.** Comparison of fruit development among treatments. (**a**) Litchi fruit numbers during fruit drop period; (**b**) single litchi fruit weight during fruit development.

Figure 5b illustrates the relative growth rate patterns of fruits across treatments. Notably, litchi fruit growth followed a typical exponential growth curve in which three developmental stages (S1–S3) can be clearly recognized after fruit drop period [26]. Stage I is primarily characterized by the growth of pericarp and seed. Stage II is mainly characterized by the growth of an embryo. The accumulation of sample mass of fruit peel and seed is significantly faster than that of aril mass in stage II. While stage III is with the rapid aril growth and maturation (), 70% to 80% of the fresh sample weight of the aril is completed during this period. The growth dynamics of fruit weight in defoliation treatments was similar to control but with higher values, both increased rapidly after 17 May (S2 stage) and reached maximal levels on 20th June (S3 stage). The fruit weight showed a sharp increase at S3 stage. Ultimately, the fruit weight of T1 and T2 were around 20.4 g; it was significantly higher than that of control as 18.5 g, as shown in Table 1. However, the seed weight in defoliation treatment was significantly higher than that in control (Table 1), suggesting that the seed may play an important role in fruit weight changes in litchi cv. Guiwei.

Table 1 provides comparative analysis of key fruit quality parameters at maturity. Moderate defoliation (T1) significantly enhanced overall fruit quality relative to controls, demonstrating superior performance in dimensional indices (longitudinal/transverse diameter), individual fruit weight (10.3% increase), total soluble solids (TSS; unchanged), and final yield per tree (23.3% higher). Although T2 fruits exhibited comparable weights to T1, they showed significantly reduced TSS levels (1.8°Brix decrease) and decreased pulp thickness (2.1 mm reduction), indicating qualitative deterioration under intensive defoliation.

**Table 1.** Comparison of litchi fruit quality at maturity period among defoliation treatments.

| Treatment | Yield Per Tree (kg) | Fruit | | | | | Seed | |
|---|---|---|---|---|---|---|---|---|
| | | Longitudinal Diameter (mm) | Long Transverse Diameter (mm) | Short Transverse Diameter (mm) | Single Fruit Weight (g) | Thickness of Pulp (mm) | TSS | Seed Weight (g) |
| Control | 30 | 32.9 | 33.9 | 32.8 | 18.5 $^{b}$ | 10.3 $^{a}$ | 18.94 $^{a}$ | 0.64 $^{c}$ |
| T1 | 37 | 33.3 | 34.7 | 33.5 | 20.4 $^{a}$ | 10.3 $^{a}$ | 18.68 $^{a}$ | 1.25 $^{b}$ |
| T2 | 35 | 32.8 | 34.4 | 32.9 | 20.4 $^{a}$ | 8.2 $^{b}$ | 17.16 $^{b}$ | 2.43 $^{a}$ |

Note: Different letters indicate statistically significant differences between groups, at the 0.01 probability level.

Collectively, these findings demonstrated that moderate defoliation (T1) significantly improved fruit quality metrics while maintaining yield stability, whereas severe defoliation (T2) induced unbalanced quality development and overall degradation.

### *3.2. Canopy Structural Dynamics and Light Environment Variation*

To further investigate the regulatory effects of defoliation treatments on canopy architecture and their subsequent impact on imaging conditions, three key parameters were quantified across all experimental groups, including shoot curvature angle, leaf area index (LAI), and photosynthetically active radiation (PAR) within the canopy profile.

#### 3.2.1. Shoot Curvature Angle

Based on the collected data, a frequency distribution concerning the bending angle of litchi fruiting shoots was created, as shown in Figure 6.

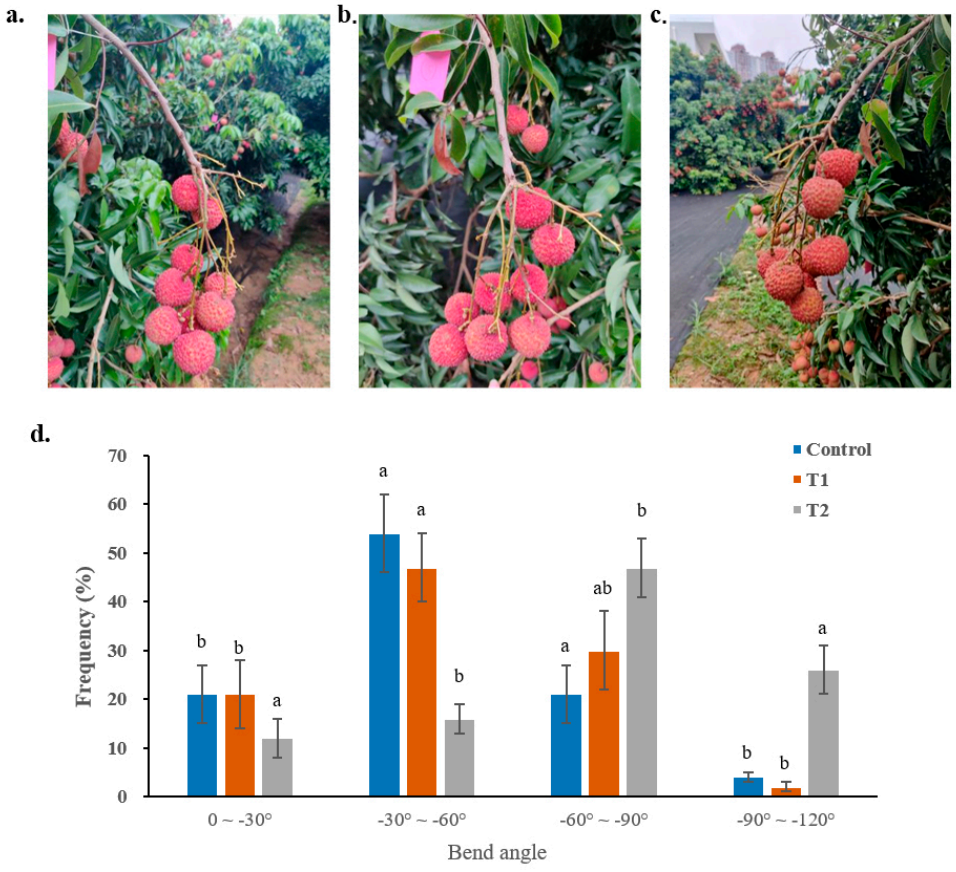



**Figure 6.** Changes in bending angle of litchi fruiting shoot. (**a**) Left side of litchi cluster; (**b**) front side of litchi cluster; (**c**) right side of litchi cluster; (**d**) frequency distribution of bending angles. Note: Different letters indicate statistically significant differences between groups.

The results showed that the proportion of shoots with bending angles in the range of −30° to −60° was the highest in control, accounting for 53.8%, followed by the range of −60° to −90°, accounting for 21.2%. The proportion of shoots between 0° and −30° was also 21.2%. Relatively, the bending angle between −90° to −120° accounted for only 3.8% in total. The average drooping angle of litchi fruiting shoots was −45.9° ± 21.6, indicating that most fruiting shoots were in a downward bending state during maturity. Interestingly, T1 showed a similar distribution of shoots with bending angles as control, but T2 had 46.5% of shoots with bending angles in the range of −60° to −90°, and 25.6% in −90° to −120°. Shoots in the intensive defoliation treatment exhibited significantly greater curvature angles than other groups ($p < 0.01$), indicating that severe leaf defoliation substantially increased shoot gravitropic responses. This architectural alteration likely exacerbated fruit occlusion within the canopy interior.

Multivariate regression analysis of bending angles against shoot structural parameters across four sampling dates yielded the following predictive model:

Bending angle = −56.054 − 22.095 × Stem thickness + 3.803 × Fruit number + 4.611 × Fruit size. The model coefficients indicate a significant negative correlation between stem thickness and bending angle ($\beta = -22.095$, $p < 0.01$), demonstrating enhanced resistance to bending in thicker shoots. Conversely, positive correlations emerged for both fruit number ($\beta = 3.803$, $p < 0.01$) and fruit size ($\beta = 4.611$, $p < 0.01$), indicating greater curvature under higher fruit loads. These results substantiated that shoot architecture was predominantly governed by fruit loading dynamics. Intensive defoliation likely exacerbated bending deformations through concentrated fruit distribution, consequently impairing fruit visibility within the canopy.

#### 3.2.2. Canopy Light Intensity and LAI Dynamics

Fruit visibility in imagery is influenced not only by morphological characteristics but also by synergistic effects of illumination conditions and foliar occlusion at the acquisition angle [27]. Leaf area index (LAI) and photosynthetically active radiation (PAR) serve as critical parameters for quantifying canopy structural density and light transmittance, providing indirect indicators of fruit target exposure. To systematically evaluate defoliation effects on canopy light environments and structural features, vertical profiles of LAI and PAR were measured at multiple canopy heights across treatment groups during May and June.

As shown in Figure 7, dramatic behavior in the observation period between May and June was observed with highly variable LAI and PAR.

There was a negative correlation between the leaf area index and the degree of leaf defoliation at the early stage. In May, the highest LAI value in the control litchi appeared at the bottom of the tree crown, ranged from 7.09 to 7.54, and the lowest value was around 3.1 at the top, which implied that the leaves were concentrated in the lower part of the tree crown (Figure 7a). Compared with control, the leaf area index of intense leaf defoliation in the middle of the crown decreases to 2.0–4.0, but the leaf area index at the top of the crown significantly decreased to around 1.0–3.0 (Figure 7a). As a result, in May, light damage in T2 happened because of excessive light. Additionally, the LAI value of T1 exhibited a little change from the bottom to the top of the tree crown, as only the middle part of the crown was slightly higher (Figure 7a).

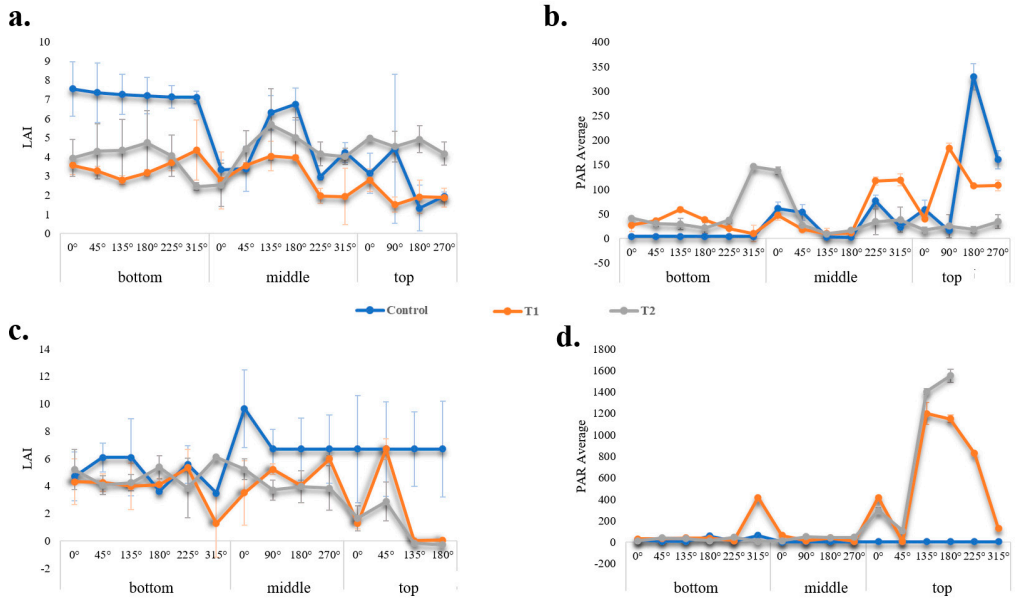



**Figure 7.** Comparison of light intensity and LAI of litchi canopy. (**a**) LAI in May; (**b**) light intensity in May; (**c**) LAI in June; (**d**) light intensity in June.

While in June, despite the fruiting branches gradually drooping, the leaves were still present and abundant in the control; therefore, the LAI value significantly increased to 7.19 ± 1.21 in the middle of the tree. However, the LAI value of T1 and T2 showed little change compared to May. It would imply that the defoliation downregulated the LAI value in the middle parts of the tree crown.

PAR value was also determined in both May and June. The results are shown in Figure 7b,d. In May, T2 improved the PAR at the middle and bottom of the tree. Meanwhile, T1 improved the PAR at the middle and top of the tree, which was consistent with the above LAI result (Figure 7b). The defoliation treatment significantly increased the light intensity in the crown. In June, there was significant difference between control and treatments. The defoliation treatments strongly increased the light intensity at the top of the tree with higher PAR value (Figure 7d).

Collectively, moderate defoliation (T1) successfully enhanced irradiance conditions within fruit-bearing canopy zones and optimized imaging environments without compromising structural integrity. In contrast, intensive defoliation (T2), while further reducing LAI by 41.7% and elevating PAR to 44 μmol·m$^{-2}$·s$^{-1}$ at the middle, induced significant trade-offs through detrimental effects on shoot architecture and fruit quality attributes.

### *3.3. Fruit Target Detection Performance Analysis*

#### 3.3.1. Experimental Configuration

To ensure a fair comparison of algorithm performance, identical training platforms and hyperparameter configurations were employed. The hardware and software specifications were as follows: An Intel Xeon Gold 6256 CPU (3.60 GHz, 48 physical cores, 24 threads; manufactured by Intel Corporation, Santa Clara, CA, USA) with 1024 GB RAM, and an NVIDIA RTX A6000 GPU (48 GB VRAM) were utilized. The system operated under Ubuntu 18.04, with CUDA 11.8.130, cuDNN 8.6.0, NVIDIA driver 535.104, OpenCV 4.8.0, and PyTorch 2.0.1. The YOLOv8 architecture was implemented with the following hyperparameters: input image resolution = 640 × 640 pixels, training epochs = 200, batch size = 16, optimizer = AdamW, initial learning rate = 0.01, momentum = 0.937, and weight decay = 5 × 10$^{-4}$.

3.3.2. Cross-Model Detection Performance Evaluation

The performance of the detection network largely determines the effectiveness of subsequent tasks such as fruit yield estimation. In this section, a comparative experiment was designed to verify the effectiveness of the proposed detection algorithm. For a fair baseline comparison, all models were trained and evaluated on the control (CK) dataset without defoliation. This ensured that the performance differences reflected only the inherent capability of each network architecture, independent of treatment effects. The experimental comparison models include YOLOv5, YOLOv7, and YOLOv8.

As shown in Table 2, in terms of model accuracy, the precision, recall, and mAP values of YOLOv8 are 0.835, 0.826, and 0.868, respectively. The mAP value was 6.77% and 5.08% higher than YOLOv5 and YOLOv7, respectively, compared to the same period last year. In terms of real-time performance, YOLOV8 has a single frame inference time of 160.3, which was shorter than YOLO v5's 172.5 and YOLO v7's 178.6. The experimental results indicated that the litchi detection model based on YOLOv8 network had better detection performance.

**Table 2.** Comparison of different detection network performance.

| | **Precision (P)** | **Recall (R)** | **mAP** | **Inference Time/ms** |
|---|---|---|---|---|
| YOLOv5 | 0.85 | 0.745 | 0.813 | 172.5 |
| YOLOv7 | 0.833 | 0.808 | 0.826 | 178.6 |
| YOLOv8 | 0.835 | 0.826 | 0.868 | 160.3 |

3.3.3. Comparative Analysis of Detection Performance with and Without Defoliation Treatment

To evaluate whether moderate defoliation significantly enhances fruit recognition accuracy, we selected the optimal treatment group (T1) based on prior agronomic trait and light-structure analyses. A UAV image dataset was constructed using the highest-performing YOLOv8 model for comparative assessment against the control group (CK). Experiments were conducted at the Guangdong Academy of Agricultural Sciences lychee demonstration orchard using uniformly managed 'Guiwei' litchi trees. Figure 8 illustrates detection outcomes across treatment groups. Untreated canopies (Figure 8a,b) exhibited substantial missed detections due to severe foliar occlusion, particularly affecting small (≤25 mm diameter) and partially obscured fruits.

Conversely, T1-treated trees demonstrated significantly enhanced fruit exposure, enabling more precise fruit boundary localization and higher overall detection completeness (Figure 8c,d).

The specific quantitative results are shown in Table 3. When the experimental objects were fruit trees without leaf defoliation processing, the accuracy, recall, mean average precision (mAP), and F1 value of the model were 0.787, 0.805, 0818, and 0.796, respectively. On the contrary, the accuracy, recall, mean average precision (mAP), and F1 value of the model were increased to 0.846, 0.839, 0.884, and 0.842, respectively, with the objects with leaf defoliation processing. These results demonstrated that suitably enhanced fruit distinctiveness in images significantly improved the accuracy and completeness of fruit detection, thereby providing a robust foundation for subsequent orchard yield estimation and harvesting path planning.

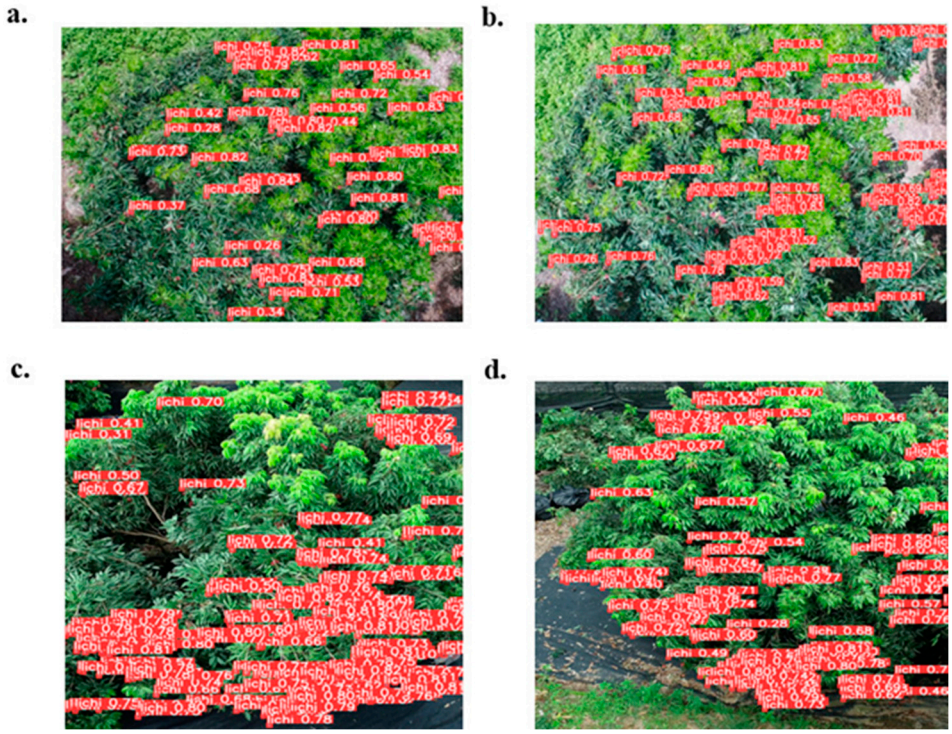



**Figure 8.** Model detection effect diagram with or without defoliation treatment. (**a**,**b**) Detection effect of litchi trees without defoliation treatment; (**c**,**d**) detection effect of litchi trees with moderate defoliation treatment (T1).

**Table 3.** Comparison of detection effects with and without defoliation treatment.

| | Precision (P) | Recall (R) | mAP | F1 |
|---|---|---|---|---|
| Control | 0.787 | 0.805 | 0.818 | 0.796 |
| T1 | 0.846 | 0.839 | 0.884 | 0.842 |

## 4. Discussion

This study demonstrates that moderate defoliation during early fruit development significantly improves canopy light distribution and fruit visual discernibility in imagery, resulting in enhanced target detection performance without compromised yield. Although both moderate (T1) and intensive (T2) defoliation induced initial fruitlet abscission, trees exhibited substantial compensatory capacity during subsequent development, resulting in statistically equivalent final fruit settings across treatments. Compared to controls, T1 and T2 fruits showed significantly higher single fruit weights (+10.3%; $p < 0.01$) and seed mass, indicating preferential photoassimilate allocation to reproductive structures, despite reduced leaf competition. This aligns with established models where seed development governs fruit mass variation [28]. Moderate defoliation optimized light penetration and spatial homogeneity without inducing significant shoot curvature. T1 reduced mid-upper canopy leaf area index (LAI) by 32.4% ($p < 0.01$) while increasing photosynthetically active radiation (PAR) by 47.7% (±5.2 $\mu mol \cdot m^{-2} \cdot s^{-1}$), structurally mitigating fruit occlusion. Conversely, intensive defoliation (T2) caused excessive LAI reduction (41.8%) but increased shoot bending angles by 23.6°, exacerbating occlusion through pendulous architecture.

YOLOv8-based fruit detection models confirmed these effects: T1 achieved significant improvements over controls in precision (+5.9%), recall (+3.4%), mAP@0.5 (+8.1%), and F1-score (+5.8%) (Table 3). Figure 8 illustrates enhanced fruit contour clarity and 37% lower missed detection rates in defoliated canopies, demonstrating that improved image

input quality directly boosts detection efficacy. Unlike prior model-centric optimization approaches, our methodology enhances detection accuracy (mAP: 0.88 vs. 0.82 in conventional systems) by modifying crop architecture, providing a viable solution for occlusion-heavy perennial crops. Future work should validate this defoliation strategy in structurally similar crops (e.g., citrus, longan) through integration with autonomous platforms, advancing horticultural perception system convergence.

While effective, manual defoliation remains labor intensive for commercial scaling. Subsequent research should 1) develop automated or chemically induced defoliation protocols compatible with standardized orchard management; 2) implement integrated approaches combining architectural optimization with adversarial training to enhance model robustness in complex environments; and 3) establish threshold values for defoliation intensity that balance detection gains with physiological sustainability.

## 5. Conclusions

This study proposed an integrated agronomic-computer vision optimization strategy for fruit detection, employing moderate defoliation during early litchi fruit development to enhance canopy architecture and light penetration. This approach fundamentally mitigates fruit occlusion issues, thereby improving target visibility at the imaging source. Validation through a YOLOv8-based detection model demonstrated significant improvements in precision, recall, mAP, and F1-score compared to non-defoliated controls.

Diverging from conventional model-centric optimizations, our methodology enhances perception quality at the data acquisition stage. This validates the efficacy of agricultural interventions for improving visual perception conditions, establishing a novel paradigm for overcoming target recognition challenges in complex canopy environments. The strategy demonstrates substantial potential for precision agriculture applications.

Future research should integrate automated defoliation technology with multi-source remote sensing to extend this approach to other tree crops (e.g., citrus, longan), advancing the development of co-adaptive agri-perception systems where horticultural practices and artificial intelligence operate synergistically.

**Author Contributions:** J.W.: Data curation, Methodology, Formal analysis, Validation, Writing—original draft. M.Z.: Methodology, Visualization, Writing—original draft. Z.Z.: Investigation, Validation, Software, Writing—original draft. Z.Y.: Data curation, Investigation, Software, Writing—review and editing. B.N.: Investigation, Visualization, Writing—review and editing. D.G.: Formal analysis, Visualization, Writing—review and editing. L.C.: Software, Validation, Writing—review and editing. J.L.: Conceptualization, Methodology, Funding Acquisition, Project administration, Writing—review and editing. J.X.: Conceptualization, Formal Analysis, Resources, Supervision, Writing—review and editing. All authors have read and agreed to the published version of the manuscript.

**Funding:** This research was funded by the Department of Finance of Guangdong Province (funding number 2024-TS-2-4), the Guangdong Provincial Department of Science and Technology (funding number 2023A0505050130), and the Hainan Provincial Natural Science Foundation (funding number 325MS129).

**Data Availability Statement:** The original contributions presented in this study are included in the article. Further inquiries can be directed to the corresponding authors.

**Conflicts of Interest:** The authors declare no conflicts of interest.

## References


1. Qi, W.; Chen, H.; Luo, T.; Song, F. Development status, trend and suggestion of litchi industry in mainland China. *Guangdong Agric. Sci.* **2019**, *46*, 132–139.
2. Li, C.; Lin, J.Q.; Li, Z.; Mai, C.D.; Jiang, R.P.; Li, J. An efficient detection method for litchi fruits in a natural environment based on improved YOLOv7-Litchi. *Comput. Electron. Agric.* **2024**, *217*, 108605. https://doi.org/10.1016/j.compag.2023.108605.
3. Kamilaras, A.; Prenafeta-Boldú, F.X. Deep learning in agriculture: A survey. *Comput. Electron. Agric.* **2018**, *147*, 70–90. https://doi.org/10.1016/j.compag.2018.02.016.
4. Mbouembe, P.L.T.; Liu, G.; Sikati, J.; Kim, S.C.; Kim, J.H. An efficient tomato detection method based on improved YOLOv4-tiny model in complex environment. *Front. Plant Sci.* **2023**, *14*, 1150958. https://doi.org/10.3389/fpls.2023.1150958.
5. Sa, I.; Ge, Z.; Dayoub, F.; Upcroft, B.; Perez, T.; McCool, C. Deepfruits: A fruit detection system using deep neural networks. *Sensors* **2016**, *16*, 1222. https://doi.org/10.3390/s16081222.
6. Wang, L.; Zhao, Y.; Xiong, Z.; Wang, S.; Li, Y.; Lan, Y. Fast and precise detection of litchi fruits for yield estimation based on the improved YOLOv5 model. *Front. Plant Sci.* **2022**, *13*, 965425. https://doi.org/10.3389/fpls.2022.965425.
7. Zhou, J.; Zhang, Y.; Wang, J. A dragon fruit picking detection method based on YOLOv7 and PSP-Ellipse. *Sensors* **2023**, *23*, 3803. https://doi.org/10.3390/s23083803.
8. Tang, Y.; Zhou, H.; Wang, H.; Zhang, Y. Fruit detection and positioning technology for a *Camellia oleifera* C. Able orchard based on improved YOLOv4-tiny model and binocular stereo vision. *Expert Syst. Appl.* **2023**, *211*, 118573. https://doi.org/10.1016/j.eswa.2022.118573.
9. Apolo-Apolo, O.; Martínez-Guanter, J.; Egea, G.; Raja, P.; Pérez-Ruiz, M. Deep learning techniques for estimation of the yield and size of citrus fruits using a UAV. *Eur. J. Agron.* **2020**, *115*, 126030. https://doi.org/10.1016/j.eja.2020.126030.
10. Tan, L.; Lv, X.; Lian, X.; Wang, G. YOLOv4_Drone: UAV image target detection based on an improved YOLOv4 algorithm. *Comput. Electr. Eng.* **2021**, *93*, 107261. https://doi.org/10.1016/j.compeleceng.2021.107261.
11. Zhao, Y.; Zheng, B.; Chapman, S.C.; Laws, K.; George-Jaeggli, B.; Hammer, G.L.; Jordan, D.; Potgieter, A. Detecting sorghum plant and head features from multispectral UAV imagery. *Plant Phenomics* **2021**, *2021*, 9874650. https://doi.org/10.34133/2021/9874650.
12. Li, Y.; Bao, Z.; Qi, J. Seedling maize counting method in complex backgrounds based on YOLOV5 and Kalman filter tracking algorithm. *Front. Plant Sci.* **2022**, *13*, 1030962. https://doi.org/10.3389/fpls.2022.1030962.
13. Xiong, Y.; Zeng, X.; Chen, Y.; Liao, J.; Lai, W.; Zhu, M. An approach to detecting and mapping individual fruit trees integrated YOLOv5 with UAV remote sensing. *Preprints* **2022**, 2022040007. https://doi.org/10.20944/preprints202204.0007.v1.
14. Liu, Y.; Feng, H.; Fan, Y.; Yue, J.; Yang, F.; Fan, J.; Ma, Y.; Chen, R.; Bian, M.; Yang, G. Utilizing UAV-based hyperspectral remote sensing combined with various agronomic traits to monitor potato growth and estimate yield. *Comput. Electron. Agric.* **2025**, *231*, 109984.
15. Cruz-Grimaldo, C.; Nieves, M.; Vera, E.; Duran, M.; Morales, A.; Salazar, W.; Arbizu, C.I. Yield predictions of 'Del Cerro'cotton (*Gossypium hirsutum* L.) germplasm by multispectral monitoring in the north coast of Peru. *Chil. J. Agric. Res.* **2025**, *85*, 15–26.
16. Orlandi, G.; Matese, A.; Ulrici, A.; Calvini, R.; Berton, A.; Di Gennaro, S.F. Automated yield prediction in vineyard using RGB images acquired by a UAV prototype platform. *OENO ONE* **2025**, *59*. https://doi.org/10.20870/oeno-one.2025.59.1.8133.
17. Liang, C.J.; Liang, J.T.; Yang, W.G.; Ge, W.Y.; Zhao, J.; Li, Z.R.; Bai, S.D.; Fan, J.W.; Lan, Y.B.; Long, Y.B. Enhanced visual detection of litchi fruit in complex natural environments based on unmanned aerial vehicle (UAV) remote sensing. *Precis. Agric.* **2025**, *26*, 23. https://doi.org/10.1007/s11119-025-10220-w.
18. Lin, C.; Jiang, W.; Zhao, W.; Zou, L.; Xue, Z. DPD-YOLO: Dense pineapple fruit target detection algorithm in complex environments based on YOLOv8 combined with attention mechanism. *Front. Plant Sci.* **2025**, *16*, 1523552.
19. Teng, X.; Zhang, W.; Liu, T.; Yang, J.; Ma, M. Stff-rtdetr: A small object detection algorithm based on drone aerial photography: X. Teng et al. *J. Supercomput.* **2025**, *81*, 928.
20. Melnychenko, O.; Scislo, L.; Savenko, O.; Radiuk, P. Intelligent integrated system for fruit detection using multi-UAV imaging and deep learning. *Sensors* **2024**, *24*, 1913. https://doi.org/10.3390/s24061913.
21. Baiano, A.; De Gianni, A.; Previtali, M.A.; Del Nobile, M.A.; Novel, V. Effects of defoliation on quality attributes of Nero di Troia (*Vitis vinifera* L.) grape and wine. *Food Res. Int.* **2015**, *75*, 260–269. https://doi.org/10.1016/j.foodres.2015.06.007.
22. Win, N.M.; Yoo, J.; Do, V.G.; Yang, S.; Kwon, S.I.; Kweon, H.J.; Kim, S.; Lee, Y.; Kang, I.K.; Park, J. Effects of pneumatic defoliation on fruit quality and skin coloration in 'Fuji'Apples. *Agriculture* **2024**, *14*, 1582. https://doi.org/10.3390/agriculture14091582.

23. Wang, C.Y.; Bochkovskiy, A.; Liao, H.Y.M. YOLOv7: Trainable bag-of-freebies sets new state-of-the-art for realtime object detectors. In Proceedings of the IEEE/CVF Conference on Computer Vision and Pattern Recognition, Vancouver, BC, Canada, 17–24 June 2023; IEEE: Piscataway, NJ, USA, 2023; pp. 7464–7475. https://doi.org/10.1109/CVPR52729.2023.00721.
24. Huang, G.; Liu, Z.; Maaten, L.V.D.; Weinberger, K.Q. Densely connected convolutional networks. In Proceedings of the IEEE Conference on Computer Vision and Pattern Recognition (CVPR), Honolulu, HI, USA, 21–26 July 2017; pp. 2261–2269. https://doi.org/10.1109/CVPR.2017.243.
25. Zhao, M.; Li, J. Molecular events involved in fruitlet abscission in Litchi. *Plants* **2020**, *9*, 151. https://doi.org/10.3390/plants9020151.
26. Li, J.G.; Huang, H.; Huang, X. A revised division of the developmental stages in litchi fruit. *Yuan Yi Xue Bao* **2003**, *30*, 307–310.
27. Koirala, A.; Walsh, K.B.; Wang, Z. Attempting to estimate the unseen-correction for occluded fruit in tree fruit load estimation by machine vision with deep learning. *Agronomy* **2021**, *11*, 347. https://doi.org/10.3390/agronomy11020347.
28. Li, J.G.; Zhou, B.Y. Comparison on fruit development and changes in endogenous hormone contents in pericarp between large- and aborted-seeded litchi (*Litchi chinensis* Sonn. cv. Guiwei). *Plant Physiol. Com.* **2005**, *41*, 587–590.

**Disclaimer/Publisher's Note:** The statements, opinions and data contained in all publications are solely those of the individual author(s) and contributor(s) and not of MDPI and/or the editor(s). MDPI and/or the editor(s) disclaim responsibility for any injury to people or property resulting from any ideas, methods, instructions or products referred to in the content.